arXiv:1410.5175v2 [hep-ph] 23 Oct 2014

Proceedings of the Second Annual LHCP
October 27, 2014

PRODUCTION OF CHARMED MESON-MESON PAIRS AT THE LHC: SINGLE- VERSUS DOUBLE-PARTON SCATTERING MECHANISMS

RAFAL MACIULA AND ANTONI SZCZUREK [1]

Institute of Nuclear Physics PAN, PL-31-342 Cracow, Poland
and University of Rzeszów, PL-35-959 Rzeszów, Poland

ABSTRACT

We discuss hadroproduction of open charmed mesons (D^0, $D^{\pm}$, $D_S^{\pm}$) at the LHC energy $\sqrt{s} = 7$ TeV. The cross section for inclusive production of $c\overline{c}$ pairs is calculated within the $k_\perp$-factorization (or high-energy factorization) approach which effectively includes higher-order corrections. Results of the $k_\perp$-factorization approach are compared to NLO parton model predictions. The hadronization of charm quarks is included with the help of the Peterson fragmentation functions. Inclusive differential distributions in (pseudo)rapidity and transverse momentum for several charmed mesons are calculated and compared to recent results of the ALICE, ATLAS and LHCb experiments. We also take into consideration a mechanism of double charm (two pairs of $c\overline{c}$) production within a simple formalism of double-parton scattering (DPS). Surprisingly for LHC energies the DPS cross sections are found to be larger than those from the standard SPS mechanism. We compare our predictions for DD meson-meson pair production with recent measurements of the LHCb collaboration, including correlation observables. Our calculations clearly confirm the dominance of DPS in the production of double charm, however some strength seems to be still lacking. Possible missing contribution from the so-called single-ladder-splitting DPS mechanism is also discussed.

PRESENTED AT

The Second Annual Conference
on Large Hadron Collider Physics
Columbia University, New York, U.S.A
June 2-7, 2014

[1]This work was supported in part by the Polish grants DEC-2011/01/B/ST2/04535 and DEC-2013/09/D/ST2/03724 as well as by the Centre for Innovation and Transfer of Natural Sciences and Engineering Knowledge in Rzeszów.

1 Introduction

Inclusive distributions for different species of pseudoscalar D and vector D^* open charm meson have been measured recently by ATLAS [1], ALICE [2] and LHCb [3] experiments. The LHCb group has also performed more exclusive studies of correlation observables for $D\overline{D}$ pairs in the forward rapidity region $2 < y < 4$ [4].

Usually, in numerical studies of heavy quark production the main efforts concentrate on inclusive distributions. Improved schemes of standrad pQCD NLO collinear approach are state of art in this respect. On the other hand, the k_t-factorization approach is commonly used as a very efficient tool for more exclusive studies of kinematical correlations between produced particles (see e.g. [5] and references therein). In this approach the transverse momenta of incident partons are taken into account and their emission is described by the so-called unintegrated gluon distribution functions (UGDFs). This allows to construct different correlation distributions which are strictly related to the transverse momenta of incident particles.

It was concluded recently that the cross section for $c\overline{c}c\overline{c}$ production at the LHC may be very large due to mechanism of double-parton scattering (DPS) [6]. Meanwhile, the LHCb collaboration measured unexpectedly large cross section for the production of DD meson-meson pairs at $\sqrt{s} = 7$ TeV [4]. Those data sets for double open charm production have been studied differentially only within the $k_\perp$-factorization approach, where several correlation observables useful to identify the DPS effects have been carefully discussed. In order to draw definite conclusions about the DPS effects in double charm production it is necessary to estimate precisely contribution to $c\overline{c}c\overline{c}$ final state from the standard mechanism of single-parton scattering [8].

2 Inclusive single charmed meson production

The cross section for the production of a pair of charm quark – charm antiquark within the k_t-factorization approach can be written as:

$$\frac{d\sigma(pp \to c\overline{c}X)}{dy_1 dy_2 d^2p_{1t} d^2p_{2t}} = \frac{1}{16\pi^2 \hat{s}^2} \int \frac{d^2k_{1t}}{\pi} \frac{d^2k_{2t}}{\pi} \overline{|\mathcal{M}^{off}_{shell}|^2} \times \delta^2\Big(\vec{k}_{1t} + \vec{k}_{2t} - \vec{p}_{1t} - \vec{p}_{2t}\Big) \mathcal{F}_g(x_1, k^2_{1t}, \mu^2) \mathcal{F}_g(x_2, k^2_{2t}, \mu^2). \quad (1)$$

The essential components in the formula above are off-shell matrix elements for $g^*g^* \to c\,\overline{c}$ subprocess and unintegrated (transverse momentum dependent) gluon distributions (UGDF). The relevent matrix elements are known and can be found, e.g in Ref. [9]. The unintegrated gluon distributions are functions of longitudinal momentum fraction x_1 or x_2 of gluon with respect to its parent nucleon and of gluon transverse momenta k_t. Some of them depend in addition on the factorization scale μ. In contrast to the collinear gluon distributions (PDFs) they differ considerably among themselves. One may expect that they will lead to different production rates of $c\overline{c}$ pairs at the LHC. Since the production of charm quarks is known to be dominated by the gluon-gluon fusion, the charm production in hadronic reactions at the LHC can be used to verify the quite different models of UGDFs.

The hadronization of heavy quarks is done with the help of fragmentation functions technique, using the standard Peterson model [10], normalized to the proper branching fractions from Ref. [11].

In Fig. 1 we show transverse momentum distribution of D^0 mesons. In the left panel we present results for different UGDFs known from the literature. Most of the UGDFs applied here fail to describe the ALICE data. The KMR UGDF [12] provides the best description of the measured distributions. Therefore in the following we shall concentrate only on the calculations based on the KMR UGDF. In the right panel we show the uncertainties of our predictions due to the charm quark mass $m_c = 1.5 \pm 0.3$ GeV and related with the renormalization and factorization scales $\mu^2 = \zeta m_t^2$, where $\zeta \in (0.5; 2)$. The gray shaded bands represent these both sources of uncertainties summed in quadrature. In addition, the results of relevant calculations within the LO and NLO collinear approach are presented for comparison. The k_t-factorization approach with the KMR UGDF is consistent with the NLO collinear calculations.

The left panels of Fig. 2 shows transverse momentum (top) and pseudorapidity (bottom) distributions of charged pseudoscalar $D^\pm$ mesons measured by the ATLAS experiment. Overall situation is very similar as for the ALICE case except of the agreement with the experimental data points, which is somewhat worse here. Only the very upper limit of the KMR result is consistent with the ATLAS data. This is also true for the other standard collinear NLO pQCD approaches. The worse description of the ATLAS data may be

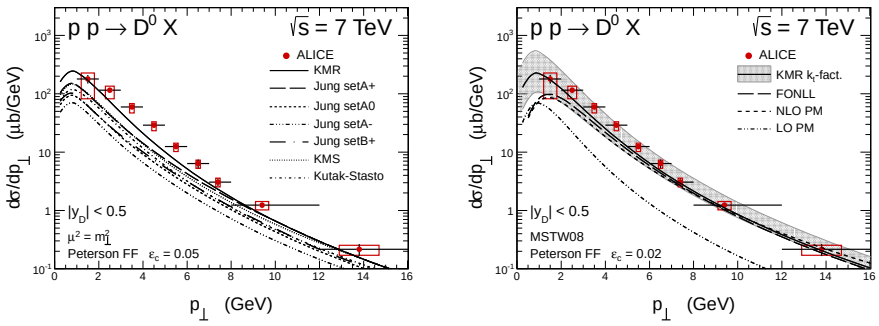

Figure 1: Transverse momentum distribution of D^0 meson for different UGDFs (left) and for the KMR UGDF compared to the pQCD collinear calculations (right) together with the ALICE data.

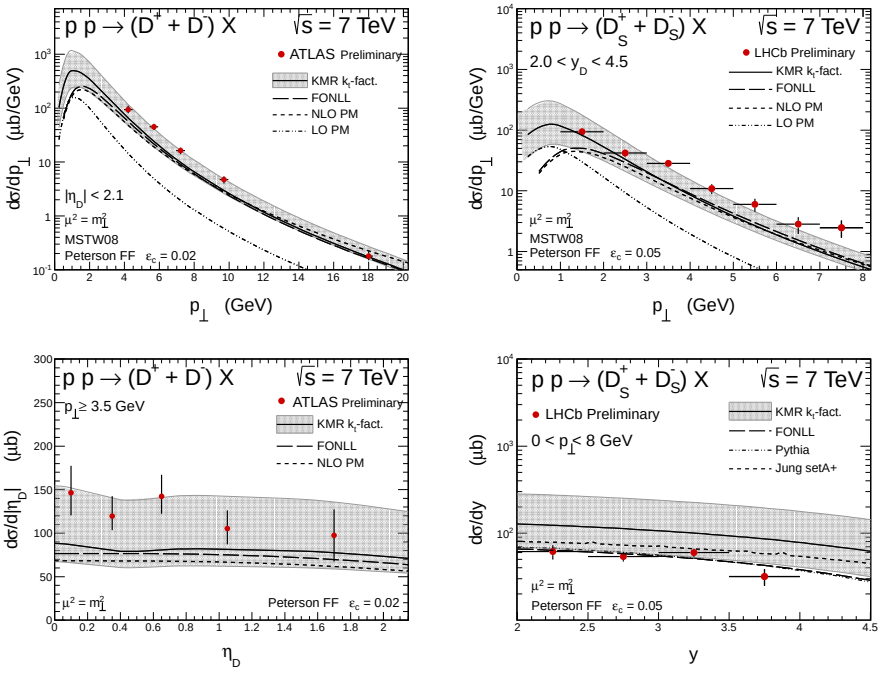

Figure 2: Transverse momentum (top) and (pseudo)rapidity (bottom) distribution of $D^{\pm}$ meson for the ATLAS experiment (left) and of $D_S^{\pm}$ meson for the LHCb experiment (right). Together with our predictions for the KMR UGDF (solid line with shaded band). Results of pQCD collinear approaches are also shown.

caused by much broader range of pseudorapidities than in the case of the ALICE detector. Potentially, this can be related to double-parton scattering (DPS) effects [7].

Recently the LHCb collaboration presented first results for the production of different D mesons in in the forward rapidity region $2 < y < 4.5$. In this case one can test asymmetric configuration of gluon longitudinal momentum fractions: $x_1 \sim 10^{-5}$ and $x_2 > 10^{-2}$. Standard collinear gluon distributions as well as unintegrated ones were never tested at such small values of x. In the right panels of Fig. 2 we present distributions corresponding to the ATLAS case but for $D_s^{\pm}$ meson. The main conclusions are the same as for ALICE and ATLAS conditions. Our results with the KMR UGDF within uncertainties are consistent (with respect to the upper limits) with the experimental data and with the NLO collinear predictions.

3 Single- and double-parton scattering effects in DD meson-meson pair production at the LHC

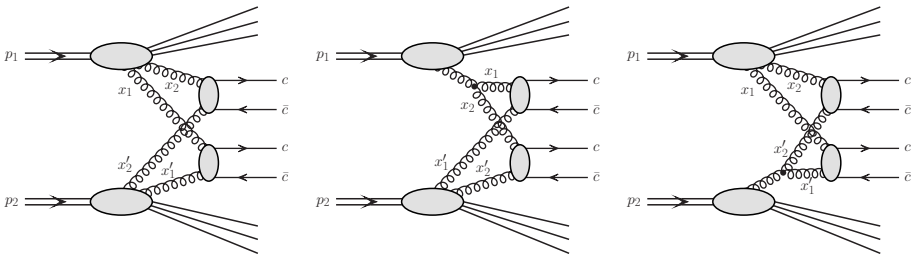

Figure 3: The standard (left) and single-ladder-splitting (middle and right) diagrams for DPS production of $c\bar{c}c\bar{c}$.

Production of $c\bar{c}c\bar{c}$ (4-parton) final state is particularly interesting especially in the context of experiments being carried out at the LHC and has been recently carefully discussed [6, 7]. The double-parton scattering formalism in the simplest form assumes two independent standard single-parton scatterings (see left diagram of Fig. 3). Then in a simple probabilistic picture, in the so-called factorized Ansatz, the differential cross section for DPS production of $c\bar{c}c\bar{c}$ system in the $k_\perp$-factorization approach can be written as:

$$\frac{d\sigma^{DPS}(pp \to c\bar{c}c\bar{c}X)}{dy_1 dy_2 d^2p_{1,t} d^2p_{2,t} dy_3 dy_4 d^2p_{3,t} d^2p_{4,t}} = \frac{1}{2\sigma_{eff}} \cdot \frac{d\sigma^{SPS}(pp \to c\bar{c}X_1)}{dy_1 dy_2 d^2p_{1,t} d^2p_{2,t}} \cdot \frac{d\sigma^{SPS}(pp \to c\bar{c}X_2)}{dy_3 dy_4 d^2p_{3,t} d^2p_{4,t}}. \tag{2}$$

This formula assumes that the two subprocesses are not correlated and do not interfere. The parameter σ_{eff} in the denominator of the above formula from a phenomenological point of view is a non-perturbative quantity related to the transverse size of the hadrons and has the dimension of a cross section. The dependence of σ_{eff} on the total energy at fixed scales is rather small and one expect, that the value should be equal to the total non-diffractive cross section, if the hard-scatterings are really uncorrelated. More details of the theoretical framework for DPS mechanism applied here can be found in Ref. [7].

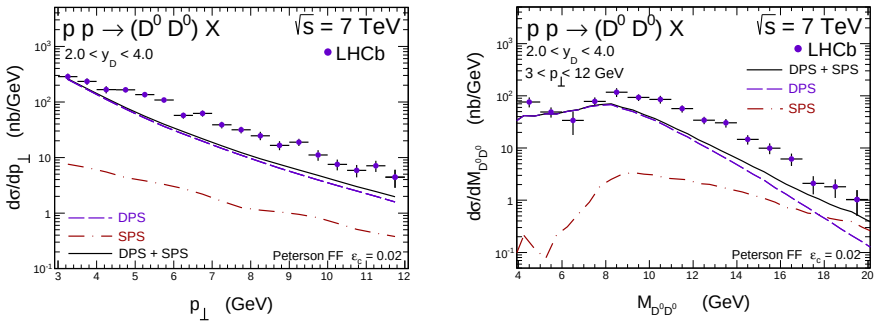

Figure 4: Distributions in meson transverse momentum when both mesons are measured within the LHCb acceptance and corresponding distribution in meson-meson invariant mass for DPS and SPS contributions.

In Fig. 4 we show distributions in meson transverse momentum (left panel) and meson-meson invariant mass (right panel). The shape in the transverse momentum is almost correct but some cross section is lacking. In the case of the DD invariant mass distribution one can also see some lacking strength at large invariant masses. In both cases, the SPS contribution (dash-dotted line) is compared to the DPS one (dashed line). The dominance of the DPS mechanism in description of the LHCb double charm data is clearly confirmed. The DPS mechanism gives a sensible explanation of the measured distribution, however some strength is still missing. This can be due to the single-ladder-splitting mechanisms discussed recently in Ref. [13].

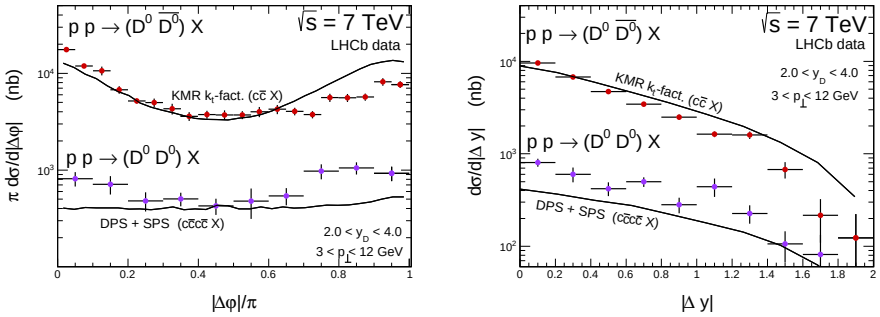

Figure 5: Azimuthal angle correlation between D^0D^0 and $D^0\overline{D}^0$ (left) and distribution in rapidity distance between two D^0 mesons and between $D^0\overline{D}^0$.

In Fig. 5 we compare correlations for D^0D^0 and $D^0\overline{D}^0$ in azimuthal angle (left panel) and in rapidity distance (right panel). In the case of the azimuthal angle distribution the experimental data suggest some small correlations at small and large angles in contrast to the flat result of the standard DPS calculation. In addition, the azimuthal angle distribution for identical mesons is somewhat flatter than that for $D^0\overline{D}^0$ which is consistent with the claim of the dominance of the DPS contribution. The rapidity distance distribution for $D^0\overline{D}^0$ falls down somewhat faster than in the case of identical D^0 mesons.

Recently, it has been found that there are (at least) two different types of contribution to the DPS cross section, which are accompanied by different geometrical prefactors ($\sigma_{eff,2v2}$ and $\sigma_{eff,2v1}$) (see e.g. [15]). One of these is the standard conventional contribution (2v2) in which two separate ladders emerge from both protons and interact in two separate hard interactions (see the left panel of Fig. 3). This is the one that is often considered in phenomenological analyses and has been applied in the studies presented above.

The other type of process is the perturbative single-ladder-splitting (2v1) which is similar to the conventional mechanism except that one proton initially provides one ladder, which perturbatively splits into two (see the middle and right diagrams in Fig. 3). Recently, the relative importance of the conventional and single-ladder-splitting DPS processes has been studied in Ref. [14].

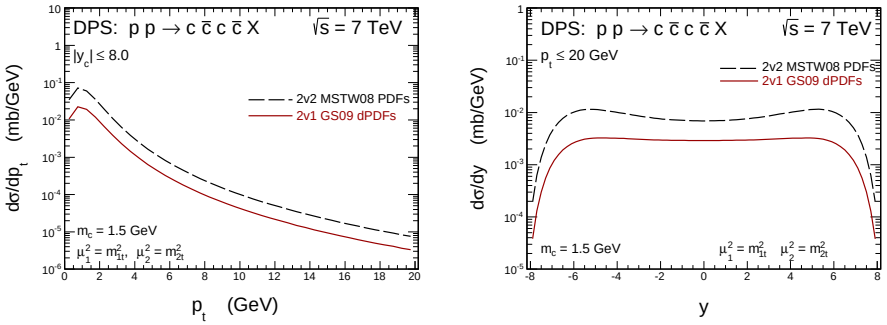

Figure 6: Transverse momentum (left panel) and rapidity (right panel) distribution of charm quark/antiquark for $\sqrt{s} = 7$ TeV for conventional and single-ladder-splitting DPS mechanisms.

In Fig. 6 we show transverse momentum (left panel) and rapidity (right panel) distribution of the charm quark/antiquark for the DPS mechanisms calculated within LO collinear approach at $\sqrt{s} = 7$ TeV. The conventional and splitting terms are shown separately. The splitting contribution (lowest curve, red online) is smaller, but has almost the same shape as the conventional DPS contribution. The ratio of the DPS single-ladder splitting contribution to the conventional one in the case of double-charm production has been roughly estimated to be at the level of $30 - 60\%$. According to these results, the missing strengths in the

description of the LHCb double charm data seem to be at least partially related to the 2v1 contribution.

The differential distributions in rapidity and in transverse momentum for the conventional and the parton-splitting contributions have essentially the same shape. This makes their model-independent separation extremely difficult. This also shows why the analyses performed are able to give reasonably good description of different experimental data sets only in terms of the conventional DPS contribution. The sum of the conventional and standard DPS contributions behaves almost exactly like the conventional contribution alone, albeit with a smaller σ_{eff} that depends only rather weakly on energy, scale and momentum fractions.

In Fig. 7 we show how the empirical (experimentally accessible) σ_{eff} value depends on centre-of-mass energy when both 2v2 and 2v1 components are taken into account (assuming that the value of $\sigma_{eff,2v2}$ is independent of energy). We see a clear dependence of σ_{eff} on energy in the plot, and also on the renormalization/factorization scales. Assuming that there is no other mechanism for an energy dependence, σ_{eff} is therefore expected to increase with centre-of-mass energy. Note also that the empirical σ_{eff} value obtained here is in the ballpark of the values extracted in experimental measurements of DPS ($15 - 20$ mb).

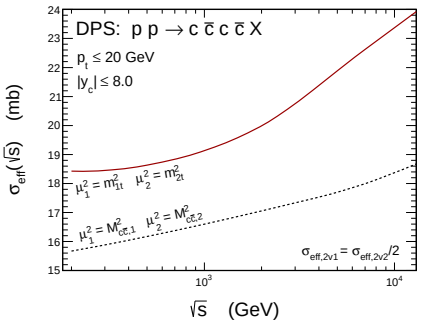

Figure 7: Energy and factorization scale dependence of σ_{eff} for $c\bar{c}c\bar{c}$ production as a consequence of existence of the 2v2 and 2v1 components. In this calculation we have taken $\sigma_{eff,2v2} = 30$ mb and $\sigma_{eff,2v1} = 15$ mb.

It is not clear in the moment how to combine the higher-order effects with the perturbative splitting mechanism. An interesting question is whether the ratio between the conventional and splitting contributions changes when higher-order corrections are included. Further studies in this context are clearly needed to fully include the splitting DPS contributions for the LHCb double charm experimental data.

References

[1] The ATLAS collaboration, ATLAS-CONF-2011-017.
[2] B.I. Abelev et al. (The ALICE collaboration), J. High Energy Phys. **01** (2012) 128.
[3] R. Aaij et al. (The LHCb collaboration), Nucl. Phys. B **871**, 1 (2013).
[4] R. Aaij et al. (The LHCb collaboration), J. High Energy Phys. **06**, 141 (2012).
[5] R. Maciuła and A. Szczurek, Phys. Rev. D **87**, 094022 (2013).
[6] M. Luszczak, R. Maciuła, and A. Szczurek, Phys. Rev. D **85**, 094034 (2012).
[7] R. Maciuła, and A. Szczurek, Phys. Rev. D **87**, 074039 (2013).
[8] A. van Hameren, R. Maciula and A. Szczurek, Phys. Rev. D **89**, 094019 (2014).
[9] S. Catani, M. Ciafaloni and F. Hautmann, Nucl. Phys. B **366**, 135 (1991).
[10] C. Peterson, D. Schlatter, I. Schmitt, P.M. Zerwas, Phys. Rev. D **27**, 105 (1983).
[11] E. Lohrmann, arXiv:1112.3757 [hep-ex].
[12] M.A. Kimber, A.D. Martin and M.G. Ryskin, Phys. Rev. D **63**, 114027 (2001).
[13] J. R. Gaunt, J. High Energy Phys. **01** (2013) 042.
[14] J. R. Gaunt, R. Maciula and A. Szczurek, Phys. Rev. D **90**, 054017 (2014).
[15] J. R. Gaunt and W. J. Stirling, J. High Energy Phys. **03**, 005 (2010).